Research Article

Heat transfer and fluid flow analysis for turbulent flow in circular pipe with vortex generator

Kishor S. Rambhad[1] · Vednath P. Kalbande[2] · Manoj A. Kumbhalkar[1] · Vivek W. Khond[2] · Rahul A. Jibhakate[2]

Received: 16 April 2021 / Accepted: 13 May 2021

Abstract

The performance of heat transfer enhancement (HTE) using modified inserts (MIs) as a vortex generator in pipe flow and fluid flow analysis using computational fluid dynamics (CFD) are evaluated in this article. The MIs are fastened to the central rod, and the circular sections of the MIs touched the circular wall of the test pipe. Heat transfer and fluid flow analyses are carried out for the various pitch to diameter ratios (P/D) and angles of the MIs. P/D ratios of 3, 4 and 6 and MIs angles of 15°, 30°, 45°, 60° and 90° are considered for experimental analysis. CFD analysis is carried out for P/D ratios of 3, 4 and 6 and MIs angles of 30°, 45° and 90°. Nusselt number (Nu/Nus) and friction factor (f/fs) ratios are evaluated using the same Reynolds number between 8000 and 17,000 in the experimental study. The MIs encourage the wall and core fluid to be combined thus helps in HTE. It is found that, as the P/D ratio increases, the Nu/Nus and f/fs decrease. If the distance between the MIs increases, the mixing of fluid weakens. With decreasing the P/D ratio, Nu/Nus increases. Increased fluid mixing leads to a higher coefficient of heat transfer and higher values of pressure drop. A P/D ratio of 4 and MIs angle of 45° results in greater heat interaction than others. Finally, recommendations for the best P/D ratio and angles of MIs are made for improved HTE on fluid flow through a circular pipe.

Article Highlights
- Modified inserts (MIs) are used inside the test pipe to check the heat transfer enhancement at various angles. Also, compared the performance with and without MIs.
- Fluid flow analysis is checked by CFD (Fluent) in Ansys software.
- Fluid flow patterns for various MIs angles and P/D ratios are compared.

Keywords Angle of modified insert · Fluid flow analysis; heat transfer enhancement · Vortex generator

Abbreviations

l	Test pipe length (m)
Um	Mean fluid velocity (m/s)
ΔP	Pressure drop (N/m^2)
f	Friction factor (-)
Q	Heat transfer rate (W)
m	Mass flow rate of fluid (kg/s)
c_p	Specific heat of fluid at constant pressure (J/kgK)
T	Temperature (°C)
h	Heat transfer coefficient (W/m^2K)
A	Area of the heated region of test pipe (m^2)
Nu	Nusselt number (-)
D	Inner diameter of the pipe (m)
k	Thermal conductivity of the fluid (W/mK)

✉ Kishor S. Rambhad, kishorsrambhad@gmail.com; Vednath P. Kalbande, v.kalbande@raisoni.net; Manoj A. Kumbhalkar, manoj.kumbhalkar@rediffmail.com; Vivek W. Khond, vivek.khond@raisoni.net; Rahul A. Jibhakate, jibhakate.rahul3@gmail.com | [1]JSPM Narhe Technical Campus, Pune, Maharashtra, India 411041. [2]G H Raisoni College of Engineering, Nagpur, Maharashtra, India 440016.

Greek symbols

P Fluid density (kg/m3)

η Heat transfer enhancement efficiency

Subscript

i Inlet

o Outlet

s Smooth test pipe/test pipe without MIs

1 Introduction

Since the coefficient of heat transfer for gas is generally lower than liquid or two-phase flow, the output of the heat exchanger is often limited to the gas side. This improvement in heat transfer performance with reduced volume and cost of production continues to inspire research in the gas side HTE. There is a market for small-size and lightweight heat exchangers for high-performance heat transferring devices. Increasing the coefficient of heat transfer or increasing the surface area, or both can have a positive impact on capital and operating costs. HTE using inserts often results in losses in terms of pressure drop (ΔP). Circular pipe inserts are the most commonly used for HTE because they are easy to build and do not require material deformation on the inside surface of the pipe. Twisted tapes (TTs) and wire coil (WC) are the most commonly used inserts [1].

Webb et al. [2] studied rib roughness characteristics in turbulent flow through the pipe. It was observed that there is boundary layer separation and reattachment, hence repeated rib surface could be seen as a problem. At the rib, separation occurs, forming a free shear layer that re-attaches downstream from the separation point at 6–8 rib height. In the vicinity of their attachment point, a maximum heat transfer coefficient occurs. The local heat transfer coefficients for the separation flow area are greater than those of an uninterrupted boundary layer. Fiebig [3] studied five different forms of plate channel heat exchangers, showing the standard plate-fin surface for gas flow. It was observed in this analysis that the VGs surface provides greater savings in the surface area of the heat exchanger and thus in the volume of the heat exchanger. Manglik and Bergles [4] established heat transfer and ΔP correlations for laminar and turbulent regimes with TTs inserts. The formation of correlation is focused on various effect. Eiamsa-ard [5] studied the heat transfer and friction characteristics in a horizontal double heat exchanger with and without TT inserts. It was observed that the best improvement for heat transfer is a single continuous tape than discontinuous tape strips as an insert. Naphon and Suwagrai [6] performed experiments using TTs, they reported that the heat transfer rate was lower than the ratio of TT pitch to higher diameter. Nag and Rao [7] reported heat transfer data for the WC insert and suggested the same correlation. For WC inserts & TT, Wang and Sunden [8] presented a performance comparison. It was found that WC inserts provide greater overall performance than TT inserts with the same helix angle and thickness ratio also WC have much lower ΔP than TT inserts. For HTE over flat surfaces, VGs namely delta wing, rectangular wing, delta-winglet pair and rectangular winglet pair were used and compared their performances by Fiebig et al. [9], delta wings have been reported to provide the greatest HTE per unit area. Yakul et al. [10] used tape in a round tube with delta-winglets-VGs on either side of the tape insert, they reported that by increasing winglet height, the Nusselt number increases slightly, but the friction factor also increases sharply by increasing winglet height and ring sector insert angle. Akhavan-Behabadi et al. [11] studied forced convective evaporation characteristics of ΔP in heat transfer in horizontal tubes with WC inserts. The helical WC with different coil pitches of 0.5, 0.8, 1 and 1.3 cm and different wire diameters of 0.05, 0.07, 0.1 and 0.15 cm were developed and the test pipe was used at full length. For the plain tube and each inserted tube, several trials were performed for several fluid velocities and heat fluxes. The analysis of the data collected showed that the WC inserts increases the heat transfer coefficient, but it leads to higher ΔP. Rambhad et al. [12, 13] studied the HTE performance using aluminium WC in evacuated glass tube used as an absorber in parabolic trough solar collector, researchers also compared the heat transfer performance through test pipe with and without WC. Huang et al. [14] improve core flow heat transfer by a porous medium insert in a tube. Naphon and Suchana [15] examined HTE and ΔP in the horizontal concentric tube with twisted wire brush inserts. The analysis of HTEs with TT inserts located separately from the tube wall was carried out by Bas and Ozceyhan [16]. Salam et al. [17] used rectangular-cut TTs as an insert to study HTE in the pipe. Eiamsa-Ard and Kiatkittipong [18] used TiO_2/water nanofluid along with multiple TT inserts for HTE in the pipe. In tubes based on genetic algorithm and CFD, Zheng et al. [19] studied HTE using porous insert configurations. Haskins and El-Genk [20] studied CFD analysis and correlation of concentration and helically shell-side ΔP. Meinicke et al. [21] investigated single-phase hydrodynamics and conjugate heat transfer in solid sponges using scale-resolved CFD modelling. Sharifi et al. [22] used CFD analysis to investigate the effects of helical WC inserts on heat transfer and ΔP in a double-pipe heat exchanger. Tusar et al. [23] performed CFD analysis of HTE and fluid flow analysis. A CFD analysis was carried out by Pandey et al. [24] for

HTE and flow characteristics of a circular tube heat exchanger using a Y-shaped insert. Dang and Wang [25] studied convective HTE mechanisms in a circular tube with a twin coil type insert. Wijayanta et al. [26] and Chokphoemphun et al. [27] investigated HTE of internal flow using punched delta winglet vortex generators (PDWVGs), PDWVGs provide higher heat transfer and pressure loss than plain tube was observed. The hydro-thermal efficiency of rectangular winglet vortex generators (RWVGs) was tested numerically and experimentally by Liu et al. [28], the results indicate that the RWVGs can agitate the cold fluid from the central flow area to the tube wall, thus improving the mixing of hot and cold fluids. Awais and Bhuiyan [29] Summarized the HTE and ΔP using Delta winglet vortex generators provide better thermal output than rectangular type, found Optimum angle of attack of 30° and 45° for HTE. Gallegos and Sharma [30] provides a review on the use of flexible plates i.e., flags as vortex generators inside a channel for HTE technology. Mahanthesh et al. [31] investigates the heat transfer properties of a nanofluid flowing over a rotating disc in the presence of a magnetic field and a convective boundary condition. Rasool and Shafiq [32] used a nonlinearly settled stretching sheet/surface, line up the MHD, heat sink/source, and convective boundary conditions in chemically reactive radiative Powell–Eyring nanofluid flow through Darcy tube. The effects of binary chemical reaction, thermal radiation, and Soret–Dufour effects on a constant incompressible Darcy–Forchheimer flow of nanofluids were studied by Rasool et al. [33].

The use of heat exchanging devices in the various application has been increased. Hence to increase the heat transfer rate is a crucial issue from a heat-saving point of view. The heat-saving challenge encourages the researcher to find an alternative to heat transfer technology. By studying the previous work, motivation for the fabrication of modified insert to enhance the heat transfer rate is developed.

The objective of the present work is to investigate HTE and fluid flow characteristics in the circular test pipe using MIs as a VGs. The use of WC, TTs, etc. as VGs for HTE is popular, but very little literature is available on the use of circumferential VGs in a circular tube. The attempt here is to get high HTE with less ΔP. Specially designed insert assemblies have been used for this purpose and results for the Reynolds number between 8000 and 17,000 are obtained.

In this paper, an experimental study is performed using MIs. Gap analysis is obtained from the exhaustive literature review which encouraged in designing MIs. Comparison of present experimental study is carried out with twisted tape insert for the validation. CFD analysis is also performed to check the flow behaviours in the test pipe with and without MIs. Finally, a conclusion is presented for heat transfer enhancement, pressure drop and fluid flow analysis.

2 Experimental setup

An experimental testing facility is built to measure the coefficient of heat transfer in a smooth and MIs-fitted pipe. As shown in Fig. 1, the Schematic of the testing facility and photograph of the test set are shown in Fig. 2.

Blower drives fluid into the test section (the air is taken as a working fluid in this study). In the test section, a venturimeter mounted before the test section measures mass flow rate and fluid velocity. To measure ΔP across the venturimeter, a U-tube manometer containing water as a manometric fluid is connected to the two pressure taps attached at the entrance and throat of the venturimeter. The ΔP in the test pipe is also measured by U-tube manometer connected across the inlet and outlet

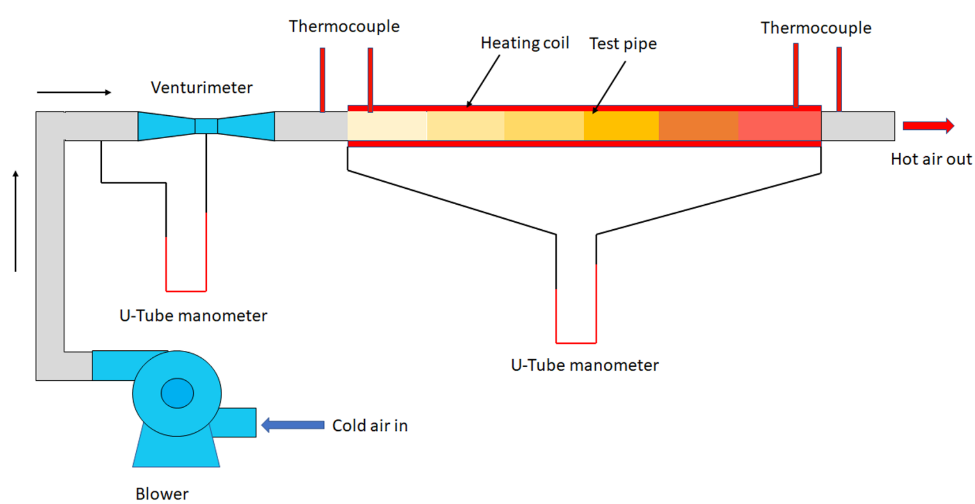

Fig. 1 Schematic diagram of the experimental setup

Fig. 2 Photograph of the experimental setup

of the test pipe. The test section is made of stainless steel pipe, has a wall thickness of 0.5 mm with 1000 mm length (l) and 25 mm inner diameter (D). The test pipe is wounded by a nichrome wire for induction heating. The heat loss to the surroundings is prevented by insulation provided over nichrome wire. The regulated power is provided to the nichrome wire via dimmer-stat, which supplies the test pipe with uniform heat flux. The fluid inlet and outlet temperatures were measured by pre-calibrated thermocouples.

The geometry of typical MIs is shown in Fig. 3a, b shows pipe fitted with MIs and Fig. 3c shows the CAD model of MIs fitted insert. Figure 4 shows the photograph of MIs fastened on a mild steel rod.

The circular geometry of the test pips has been occupied by the MIs. MIs are made from aluminium sheets 0.4 mm thick. The MIs are cut into the circular section of 25 mm diameter. At a definite axial pitch, and a definite angle from the axis of the test pipe, in the flow direction, MIs are fastened to a 3 mm mild steel rod. In the test section length (l) with the help of mean fluid velocity (Um), fluid density (ρ) and pressure drop (ΔP), the friction factor (f) is determined (as shown in Eq. 1) [17].

Fig. 4 Photograph of modified insert fitted on the central rod

$$f = \frac{\Delta p}{\rho\left(\frac{l}{D}\right)\left(\frac{Um^2}{2}\right)} \quad (1)$$

The friction factor is based on actual experimental conditions.

Heat carried (Q) by fluid flows through the test pipe is determined in terms of the mass flow rate of fluid (m), the specific heat of fluid at constant pressure (c_p), an inlet temperature of the fluid (T_i) and outlet temperature of the fluid (T_o) by Eq. 2 [17]:

$$Q = mc_p\left(T_o - T_i\right) \quad (2)$$

Average heat transfer coefficient (h) based on net heat transfer rate (Q) and area of heated region of the test pipe (A) is calculated by Eq. 3 [17]:

$$h = \frac{Q}{A\left(T_o - T_i\right)} \quad (3)$$

The Nusselt number (Nu) for fully developed flow through the test pipe with Mis is calculated in terms of heat transfer coefficient (h), an inner diameter of the pipe (D) and thermal conductivity of the fluid (k) by Eq. 4 [17]:

$$Nu = \frac{hD}{k} \quad (4)$$

For various Reynolds number, the pitch to diameter ratio and MIs angle, the experimental and CFD analysis

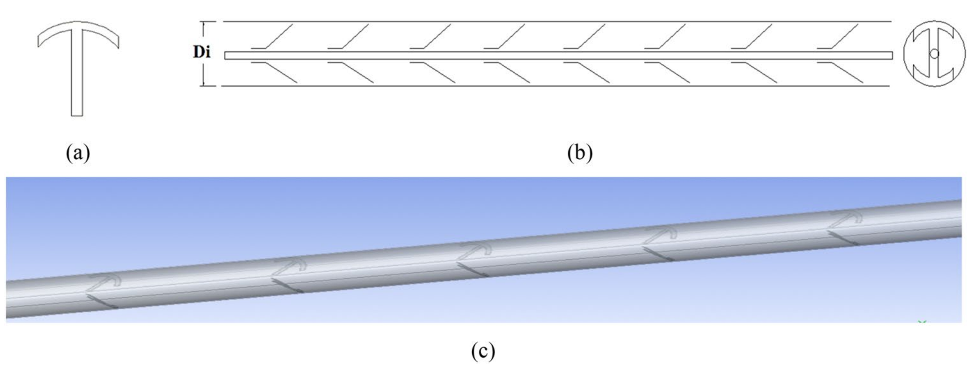

Fig. 3 **a** Modified insert **b** Pipe fitted with Modified insert **c** CAD model of MIs fitted test pipe

was carried out. The improvement of the heat transfer enhancement efficiency (η) is reported in the form of the ratio of the Nusselt number (Nu/Nus) in Eq. 5 [17].

$$\eta = \frac{Nu}{Nus} \tag{5}$$

3 Result and discussion

3.1 Experimental analysis of heat transfer enhancement

The test pipe diameter was taken as the hydraulic diameter for the fluid flow. Experimentation is performed for a fully developed flow. An experimental investigation is conducted for the various P/D ratio, various MIs angle and the various fluid flow rate. For Reynolds numbers between 8000 and 17,000 (turbulent flow), the results obtained are discussed in this paper. The results of this study are presented as the Nu/Nus and f/fs to influence the MIs performance parameter based on the same Reynolds number. Nu is the experimental value of the Nusselt number in the presence of the MIs. Nus is the experimental value of the Nusselt number of the test pipe without MIs for the same Reynolds number. f/fs is the friction factor ratio of the experimental value of the friction factor of pipe without and with MIs for the same Reynolds number. Figures 5 and 6 shows the variation of Nu/Nus and f/fs respectively for P/D = 3. Figures 7 and 8 shows the variation of Nu/Nus and f/fs respectively for P/D = 4. Figures 9 and 10 shows the variation of Nu/Nus and f/fs respectively for P/D = 6.

3.2 Validation of experimental results

To validate the present experimental results, the experimental results of test pipe fitted with MIs are compared with an experimental study carried out for twisted tape inserts by Salam et al. [17].

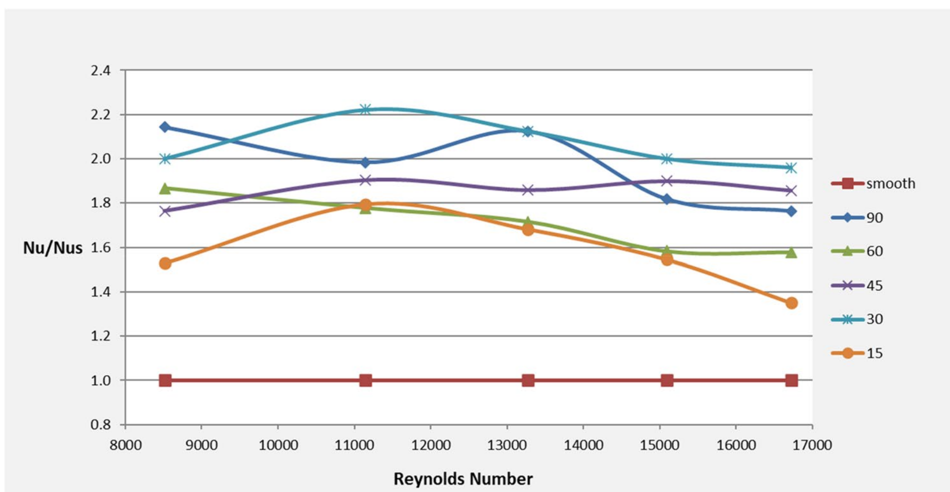

Fig. 5 Variation of Nu/Nus with Reynolds Number at P/D = 3

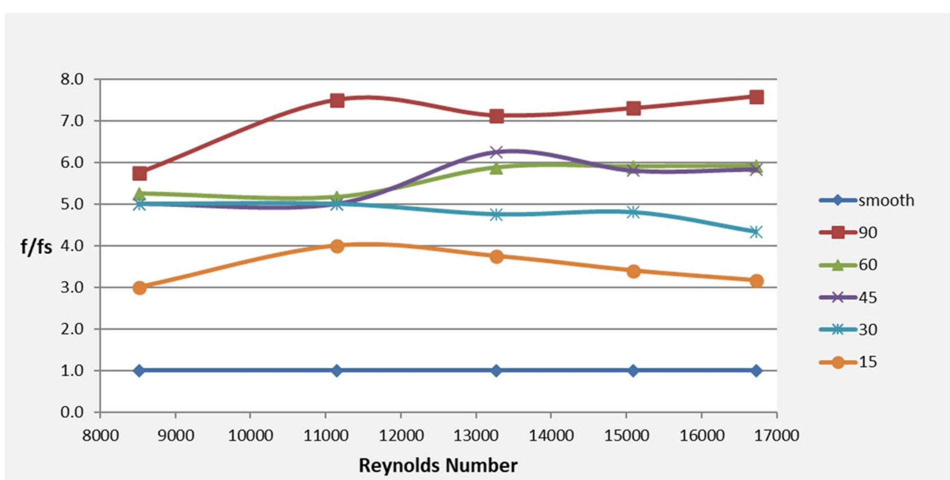

Fig. 6 Variation of f/fs with Reynolds Number at P/D = 3

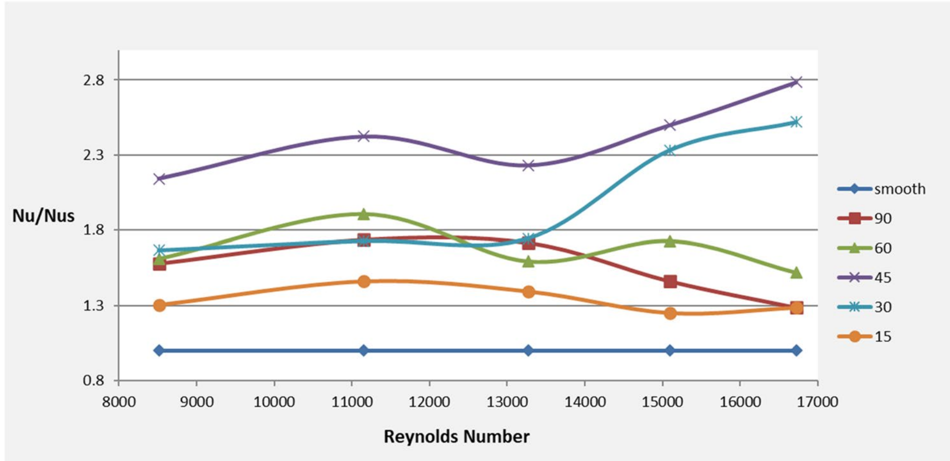

Fig. 7 Variation of Nu/Nus with Reynolds Number at P/D = 4

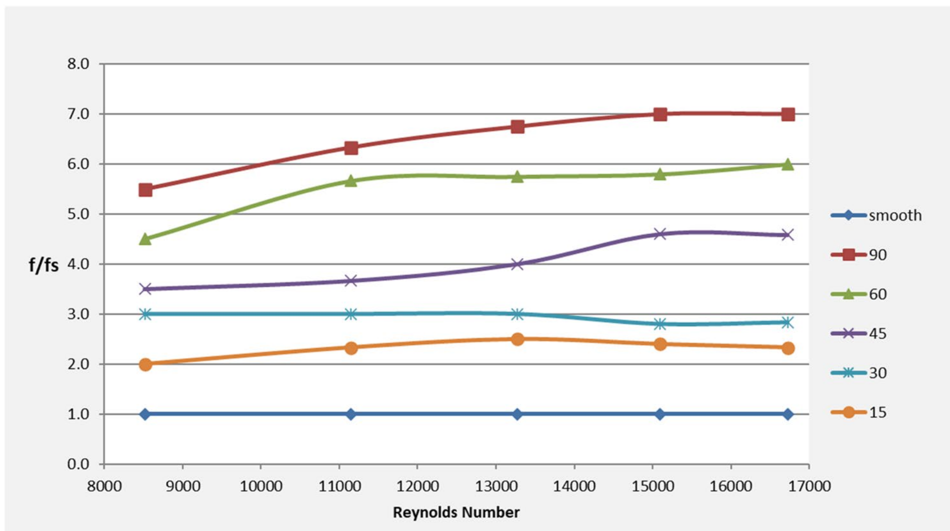

Fig. 8 Variation of f/fs with Reynolds Number at P/D = 4

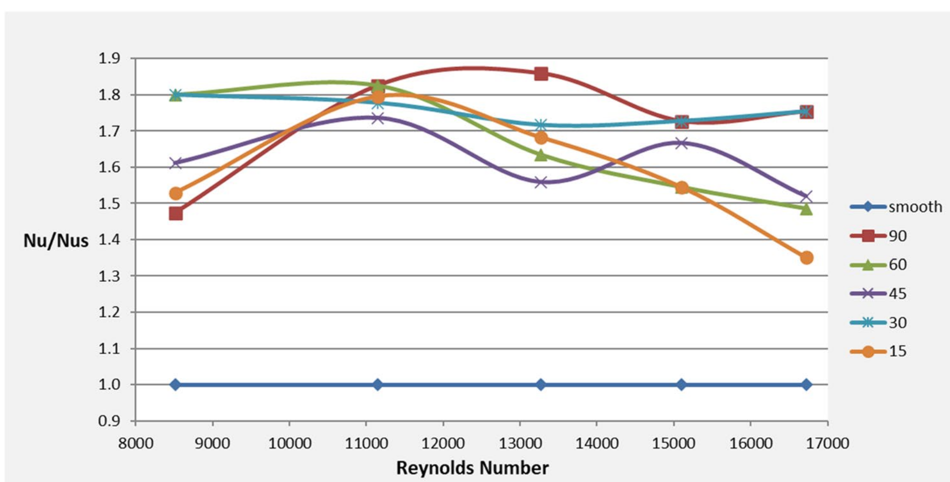

Fig. 9 Variation of Nu/Nus with Reynolds Number at P/D = 6

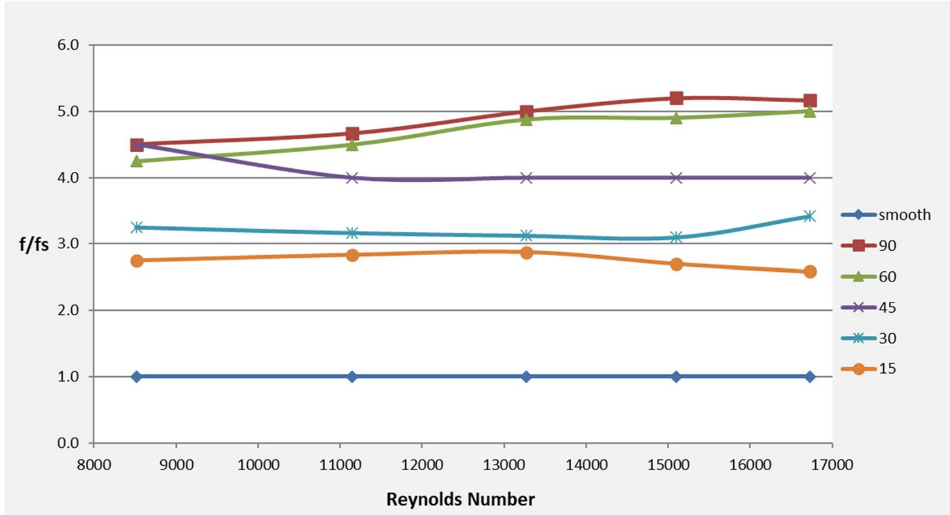

Fig. 10 Variation of f/fs with Reynolds Number at P/D = 6

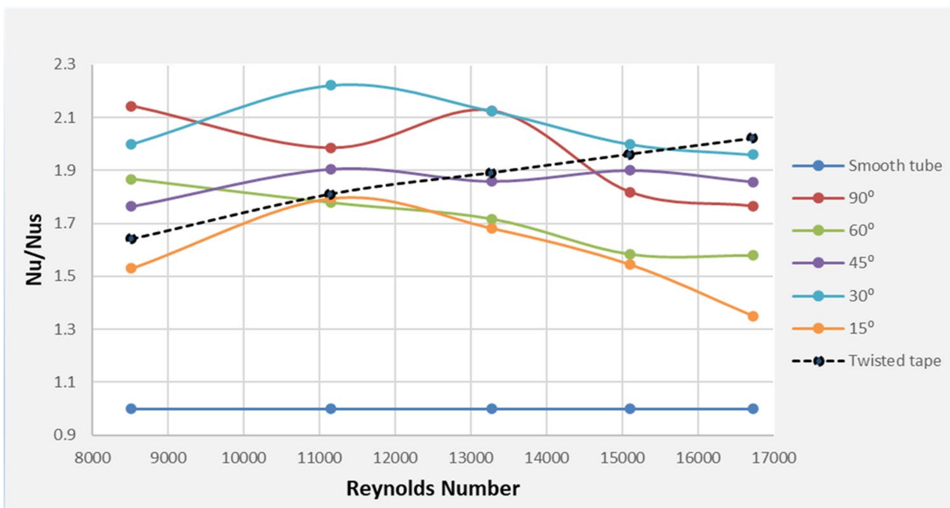

Fig. 11 Variation of Nu/Nus with Reynolds Number at P/D = 3 for MIs and Twisted tape

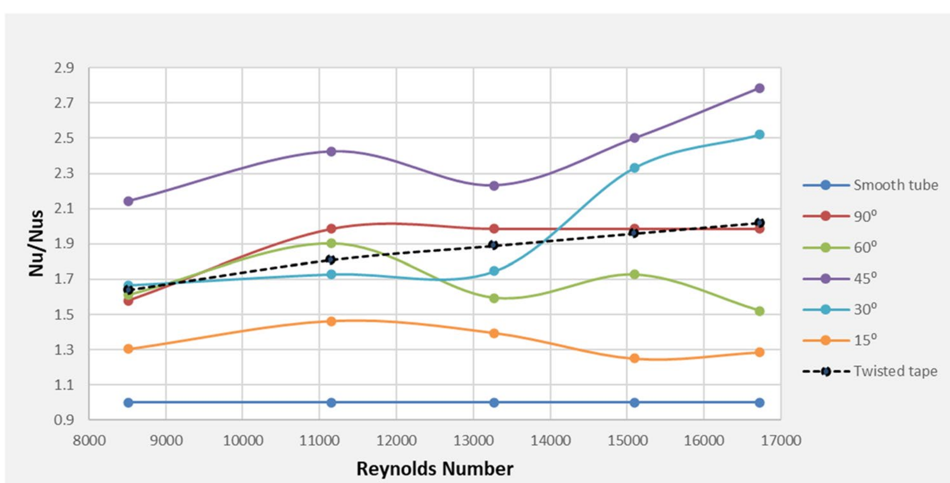

Fig. 12 Variation of Nu/Nus with Reynolds Number at P/D = 4 for MIs and Twisted tape

Figures 11, 12, 13 shows the comparison of heat transfer enhancement efficiency (Nu/Nus) for MIs and Twisted tape used by Salam et al. [17]. For twisted tape as an insert, it is observed that the Nu/Nus ratio increases as the Reynolds number increase hence twisted tape is a good alternative as an insert for a higher Reynolds Number. For MIs as an insert, it is observed that the trend of Nu/Nus ratio is different for different MIs angles and P/D ratios. Since the best result is obtained for MIs angle of 45° and P/D ratio of 4, a comparison of heat transfer enhancement using twisted tape is made with this. From Fig. 14 it is observed that, for MIs angle of 45° and P/D ratio of 4, as the Reynolds number increases Nu/Nus ratio also increase and it is much higher than twisted tape inserts for the same Reynolds number. Table 1 shows the percent improvement in heat transfer enhancement efficiency (Nu/Nus) of MIs for MIs angle of 45° and P/D ratio of 4 over the twisted tape. Hence present paper recommends the use of MIs with an angle of 45° and

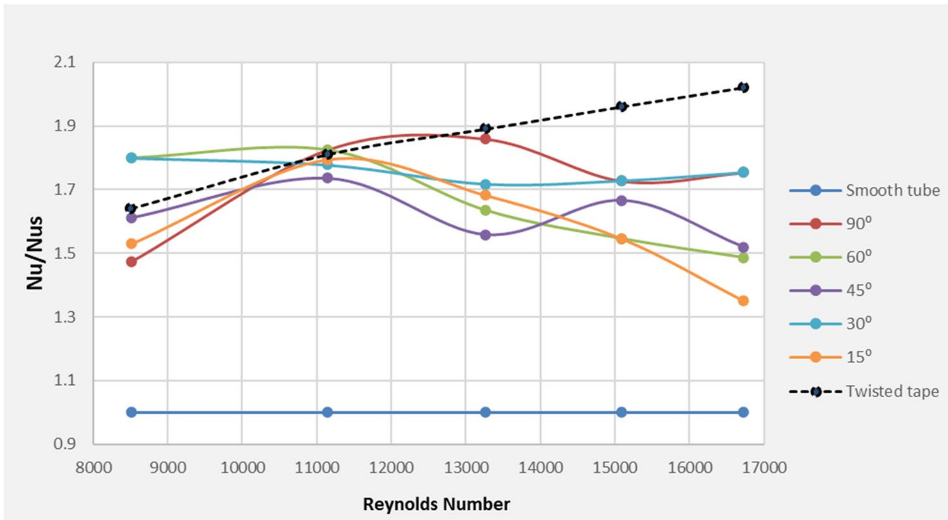

Fig. 13 Variation of Nu/Nus with Reynolds Number at P/D = 6 for MIs and Twisted tape

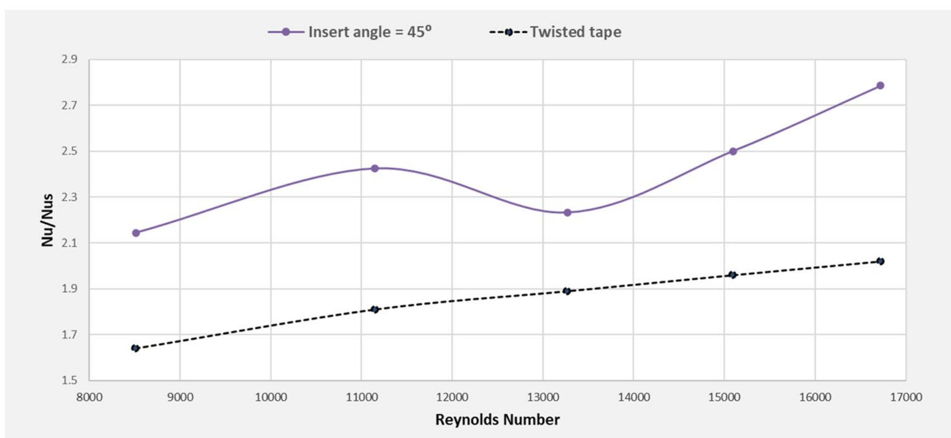

Fig. 14 Comparison of heat transfer enhancement efficiency (Nu/Nus) between MIs (MIs angle = 45° and P/D = 4) and Twisted tape

Table 1 Percent improvement of heat transfer enhancement efficiency (Nu/Nus) of MIs (MIs angle = 45° and P/D = 4) over the Twisted tape

Sr. no.	Reynolds Number	Nu/Nus (MIs)	Nu/Nus (Twisted tape)	Percent improvement in Nu/Nus of MIs over the twisted tape (%)
1	8514	2.14	1.64	30.66
2	11148	2.42	1.81	33.93
3	13269	2.23	1.89	18.05
4	15095	2.50	1.96	27.55
5	16722	2.78	2.02	37.90

P/D ratio of 4 for better heat transfer enhancement and low ΔP in a circular pipe at all ranges of Reynolds number.

3.3 Fluid flow analysis using CFD

The main difficulty in the experimental investigation is to check the fluid flow behaviour through a test pipe. Hence CFD analysis is used to check fluid flow behaviour only through the test pipe. CFD analysis is an alternative to various methods available to check fluid behaviour and it is readily available in various software. Hence, to study the behaviour of fluid flow in the test pipe with and without MIs, CFD (Fluent) tool is used in the Ansys software. Ansys 2019 R3 version is utilized for fluid flow analysis. Fluid flow analysis using CFD is performed for test pipe with and without MIs. MIs is considered for P/D ratios of 3, 4 and 6 and angles of MIs of 90°, 45° and 30°. The average values of experimental analysis for velocities, temperatures and pressures are taken for CFD analysis.

Table 2. shows the results of CFD analysis for fluid flow and heat transfer. Table 3. shows the fluid flow pattern through the pipe with and without MIs in the form of streamlines.

From Tables 2 and 3 it is observed that temperature increases from inlet to outlet gradually. Wall fluid absorbs heat from the test pipe first, then the core fluid absorbs heat from its adjacent hot layer of fluid. Cold fluid enters the test pipe, as it progresses in the test pipe cold fluid gets heated.

The velocity of the fluid in the smooth pipe is uniform throughout near the wall of the pipe but the velocity of fluid flowing through the core of the pipe increase first then decrease. When the fluid flowing through the pipe fitted with MIs, the velocity of the fluid is very less (sometimes reaches zero m/s) in the line of MIs and higher in another region.

The pressure of the fluid at the entry of the pipe is very high, but as the fluid progresses in the pipe, pressure decreases and reaches the atmospheric pressure at the outlet in the smooth pipe. But in the pipe fitted with MIs, very high ΔP was observed (sometimes fluid reaches to vacuum in the line MIs).

Flow pattern (streamlines) observed straight for the smooth pipe but as the MIs angle decreases from 90 to 30° streamlines showed a behaviour change. For MIs angles of 90° and 45° streamlines are almost the same, in these angles of MIs streamlines are straight in the vacant region and streamlines deviate in the MIs region in the test pipe. Streamlines are highly disturbed for MIs angle of 30°, streamlines move in the circular pattern while moving in the test pipe.

On the flow pattern i.e., streamlines, there is a great influence of P/D ratio and MIs angle. At MIs angle of 30°, for P/D of 3 and 4, flow is highly disturbed and swirling action observed but for P/D ratio of 6, flow is uniform and streamlines are seemed to be straight which implies increased P/D ratio recommendation for uniformed flow.

4 Conclusion

It is observed that, as the P/D ratio of the MIs increases, the Nu/Nus and f/fs decreases. The MIs encourages the wall and core fluid to be mixed. As the distance between the MIs increases, the mixing of fluid weakens. With decreasing the P/D ratio, Nu/Nus increases. Increased fluid mixing contributes to a higher coefficient of heat transfer and higher values of ΔP. A P/D = 4 results in better heat interaction than others.

Next, a fixed Reynolds number has been taken and the MIs angle is varied. As the MIs angle decreases from 90 to 15°, the Nu/Nus and f/fs decreases. Nu/Nus and f/fs increase with increasing MIs angle. With an increase in MIs angle, the Nu/Nus values indicate a small increase. The greater MIs angle implies a longer mixing zone between the core and the wall fluid, enhancing the coefficient of heat transfer. The cross-stream mixing also induces a greater ΔP. To fasten the MIs with the central rod, the projection of the MIs is necessary. This protrusion adds to the flow resistance, thus increasing the value of f/fs. This, on the other hand, increases the mixing of fluids and facilitates increased heat transfer. The best results have been obtained for optimum MIs angle values = 45° and P/D = 4.

Present experimental work is compared with twisted tape insert for the validation and authenticity of the experiment. It is observed that, MIs shown greater HTE than the twisted tape insert in the same range of Reynolds number.

Fluid flow analysis is also carried out in this work using the CFD tool. Using the CFD tool heat transfer, velocity, ΔP patterns and fluid flow behaviour are studied. Fluid flow analysis is explained in detail in the result and discussion section and related images are displayed in Tables 2 and 3. Matching results are found in HTE for experimental and CFD studies.

From the future research point of view, it is very important to consider a higher MIs angle (Maximum 90°) for HTE. In this work higher ΔP and disturbed flow pattern observed for MIs angle 30° and it would increase for MIs angle 15° further which is certainly not recommended for the future research point of view.

Table 2 Results of CFD analysis for fluid flow and heat transfer

Test pipe without MIs	Temperature variation (K)	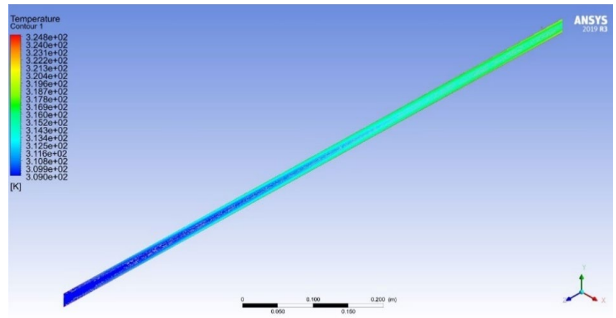
	Velocity variation (m/s)	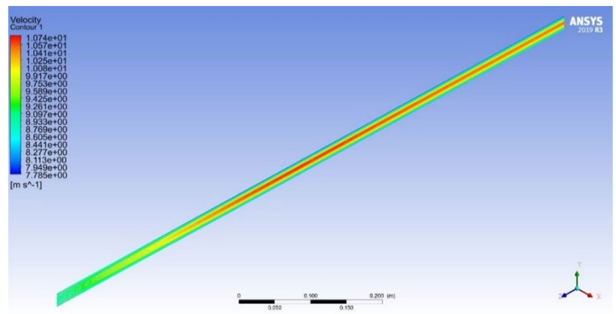
	Pressure variation (Pa)	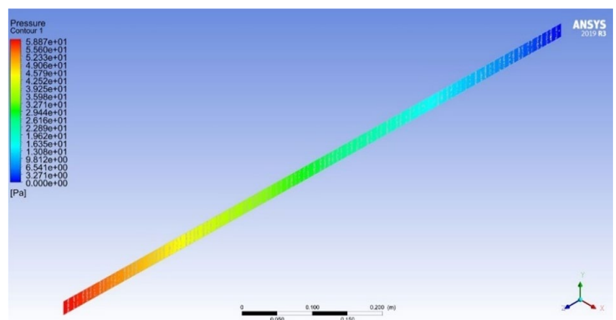

P/D ratio	MIs angle	Test pipe with MIs	
P/D = 3	90°	Temperature variation (K)	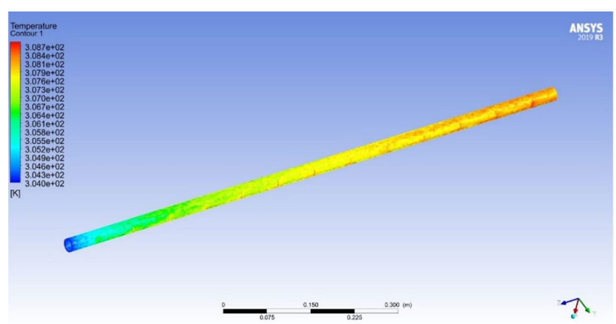

Table 2 (continued)

P/D ratio	MIs angle	Test pipe with MIs	
		Velocity variation (m/s)	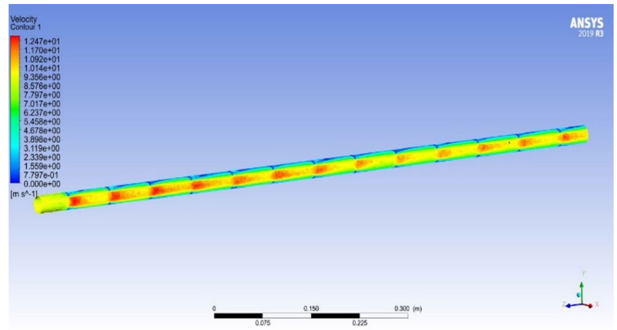
		Pressure variation (Pa)	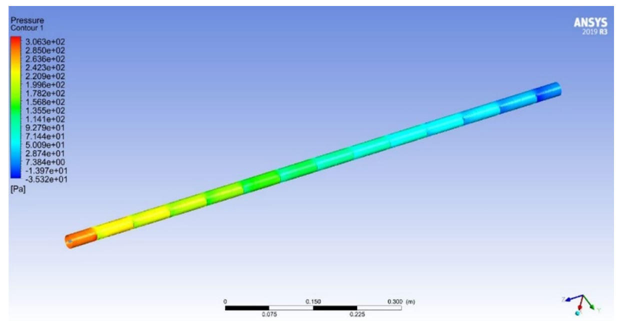
	45°	Temperature variation (K)	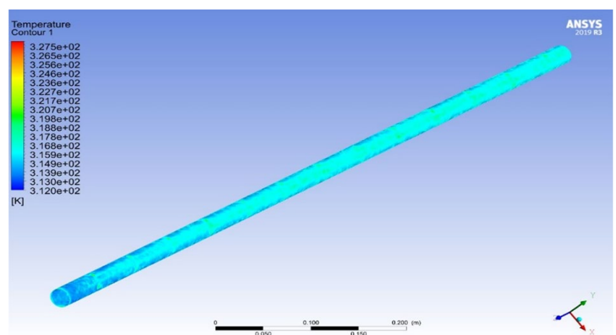
		Velocity variation (m/s)	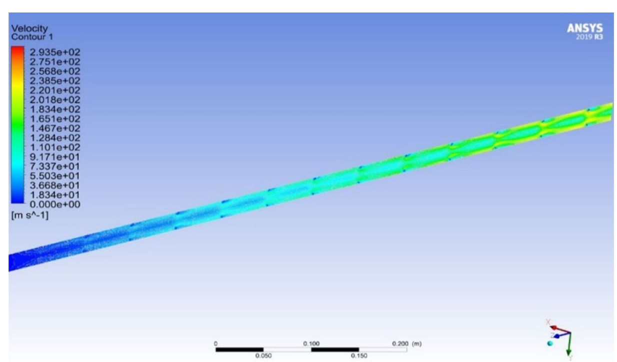

Table 2 (continued)

<table>
<tr><th>P/D ratio</th><th>MIs angle</th><th>Test pipe with MIs</th><th></th></tr>
<tr><td></td><td></td><td>Pressure variation (Pa)</td><td>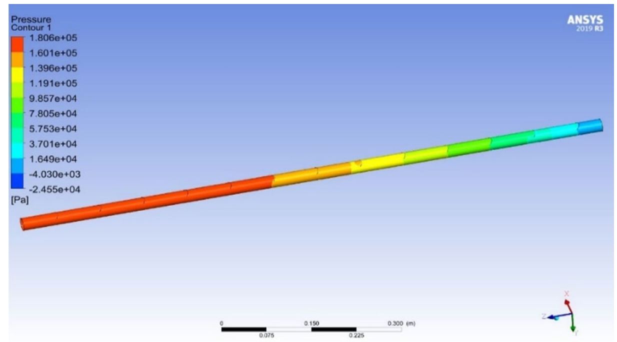
</td></tr>
<tr><td></td><td>30°</td><td>Temperature variation (K)</td><td>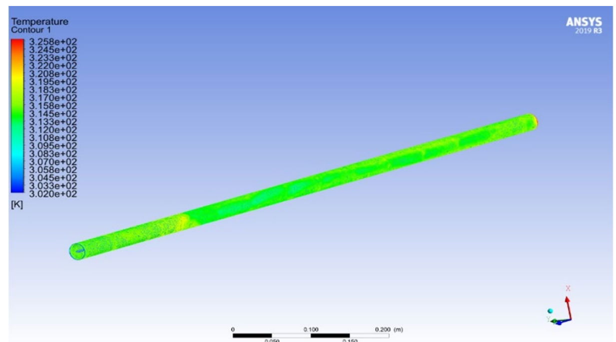
</td></tr>
<tr><td></td><td></td><td>Velocity variation (m/s)</td><td>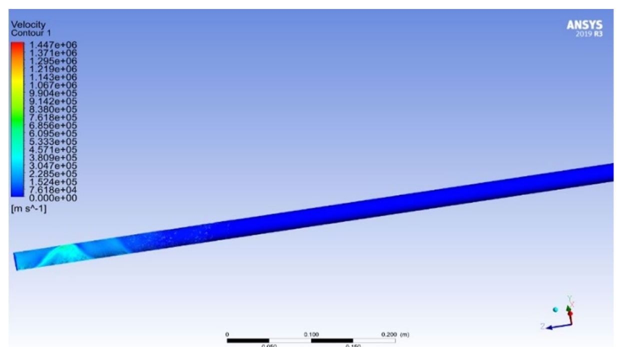
</td></tr>
<tr><td></td><td></td><td>Pressure variation (Pa)</td><td>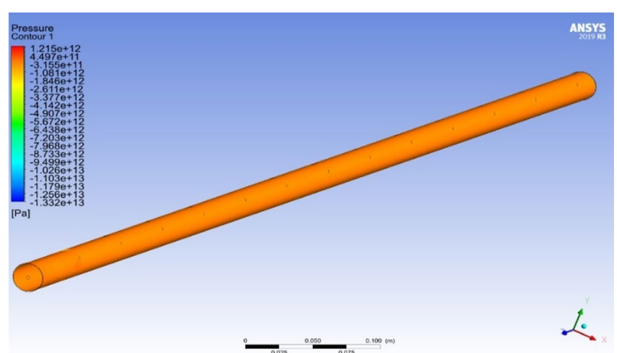
</td></tr>
</table>

Table 2 (continued)

<table>
<tr><th>P/D ratio</th><th>MIs angle</th><th>Test pipe with MIs</th><th></th></tr>
<tr><td>P/D = 4</td><td>90°</td><td>Temperature variation (K)</td><td>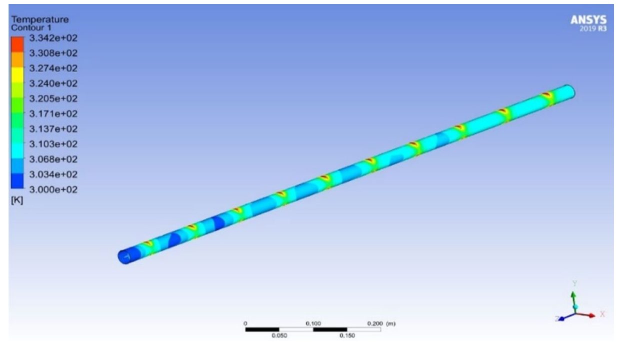
</td></tr>
<tr><td></td><td></td><td>Velocity variation (m/s)</td><td>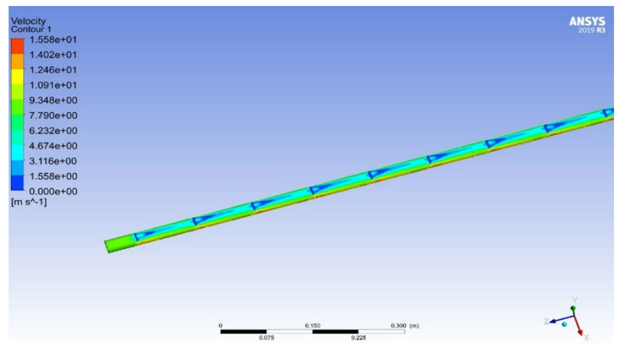
</td></tr>
<tr><td></td><td></td><td>Pressure variation (Pa)</td><td>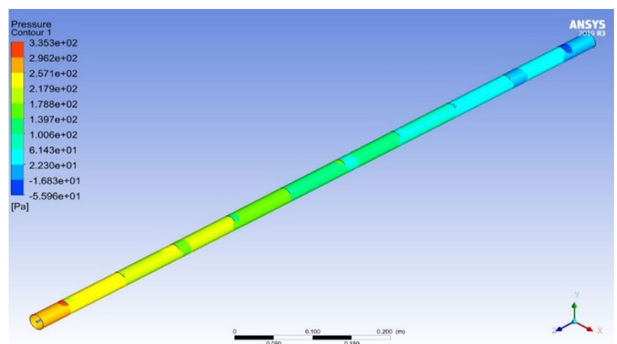
</td></tr>
<tr><td></td><td>45°</td><td>Temperature variation (K)</td><td>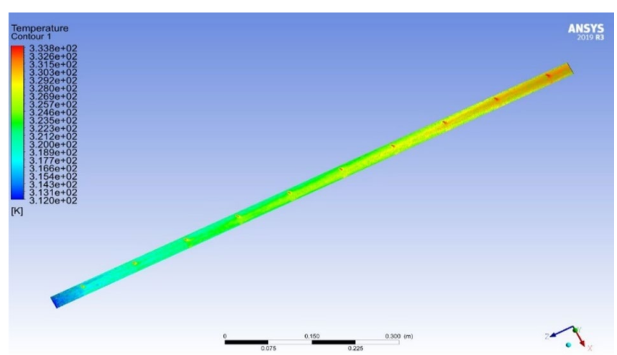
</td></tr>
</table>

Table 2 (continued)

P/D ratio	MIs angle	Test pipe with MIs	
		Velocity variation (m/s)	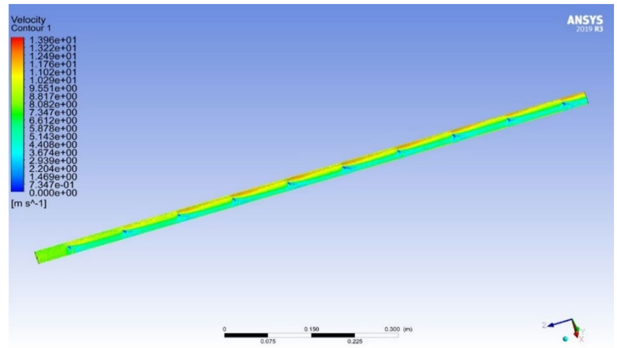
		Pressure variation (Pa)	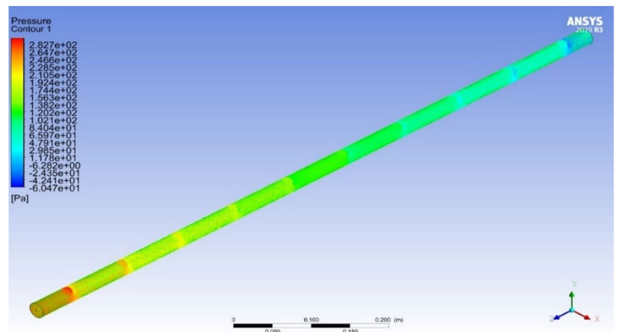
	30°	Temperature variation (K)	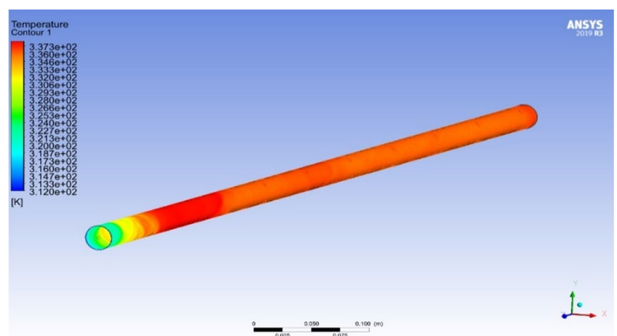
		Velocity variation (m/s)	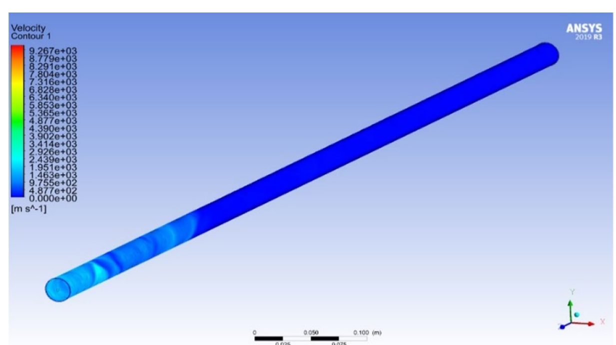

Table 2 (continued)

<table>
<tr><th>P/D ratio</th><th>MIs angle</th><th colspan="2">Test pipe with MIs</th></tr>
<tr><td></td><td></td><td>Pressure variation (Pa)</td><td>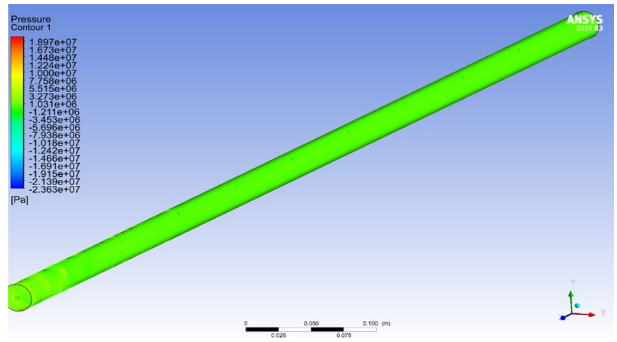
</td></tr>
<tr><td>P/D = 6</td><td>90°</td><td>Temperature variation (K)</td><td>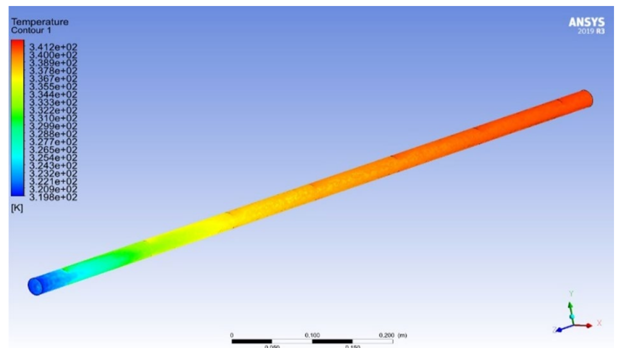
</td></tr>
<tr><td></td><td></td><td>Velocity variation (m/s)</td><td>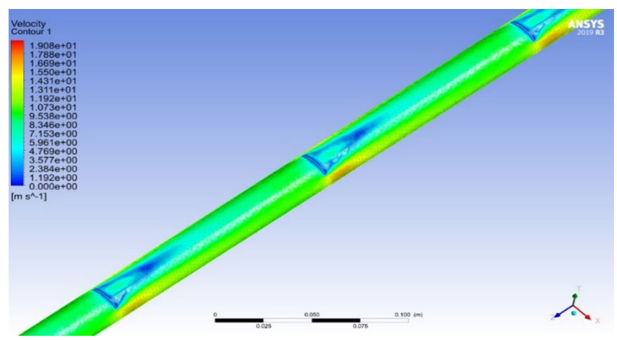
</td></tr>
<tr><td></td><td></td><td>Pressure variation (Pa)</td><td>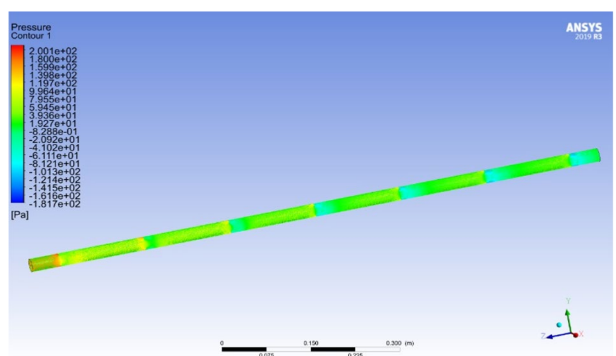
</td></tr>
</table>

Table 2 (continued)

<table>
<tr><th>P/D ratio</th><th>MIs angle</th><th>Test pipe with MIs</th><th></th></tr>
<tr><td></td><td>45°</td><td>Temperature variation (K)</td><td>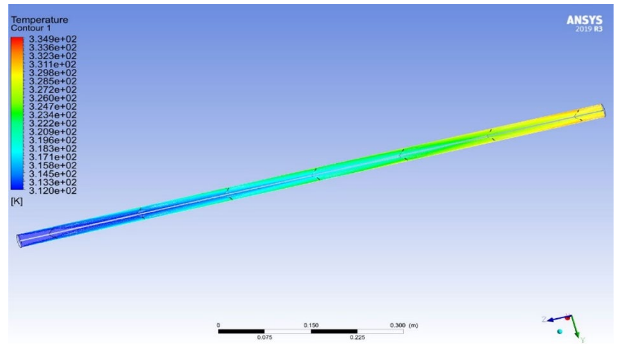
</td></tr>
<tr><td></td><td></td><td>Velocity variation (m/s)</td><td>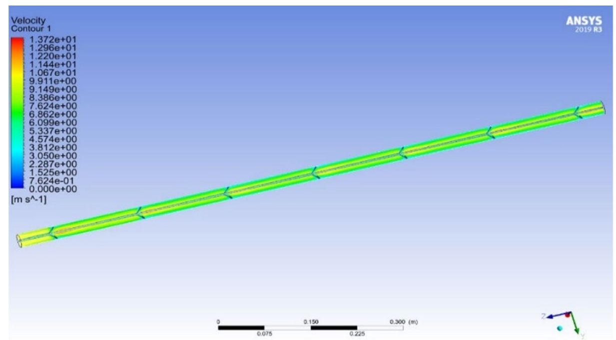
</td></tr>
<tr><td></td><td></td><td>Pressure variation (Pa)</td><td>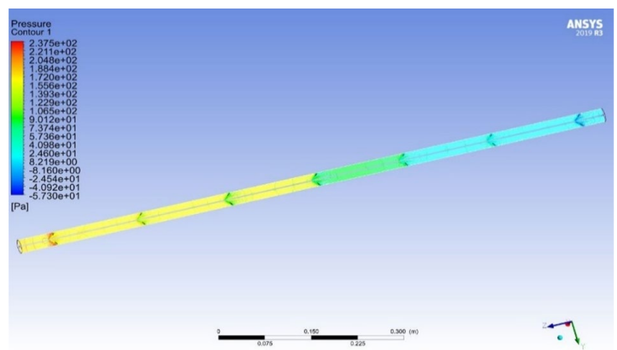
</td></tr>
<tr><td></td><td>30°</td><td>Temperature variation (K)</td><td>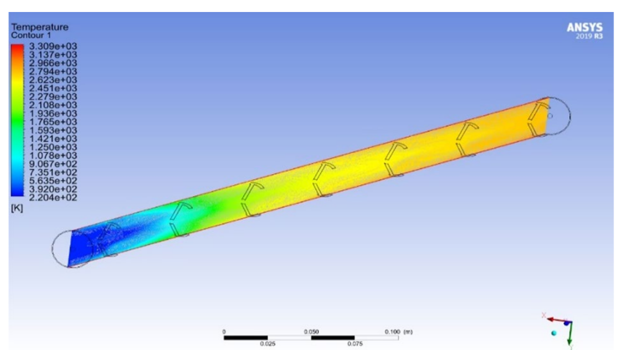
</td></tr>
</table>

Table 2 (continued)

P/D ratio	MIs angle	Test pipe with MIs	
		Velocity variation (m/s)	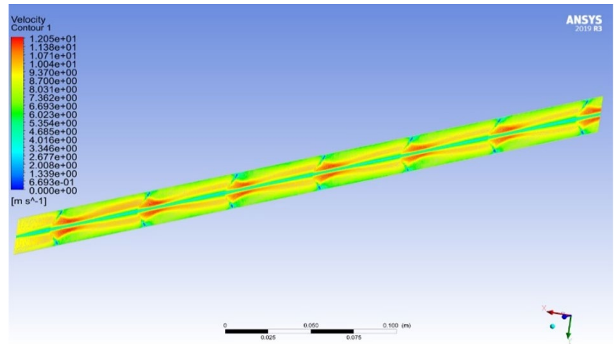
		Pressure variation (Pa)	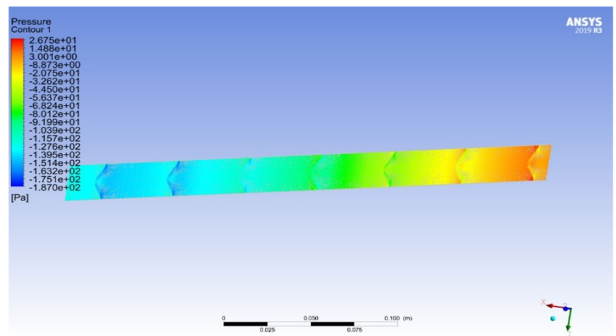

Table 3 The fluid flow pattern through the pipe with and without MIs in the form of streamlines

P/D ratio	MIs angle	
Test pipe without MIs		
Pipe without MIs		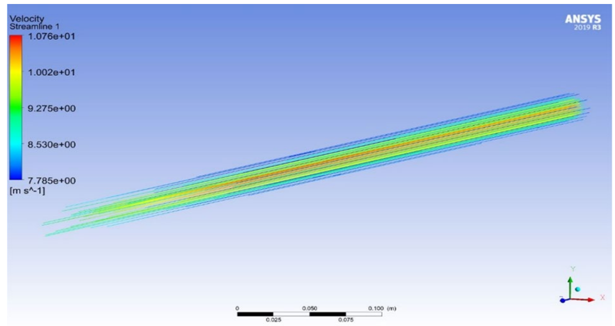
Test pipe with MIs		
P/D = 3	90°	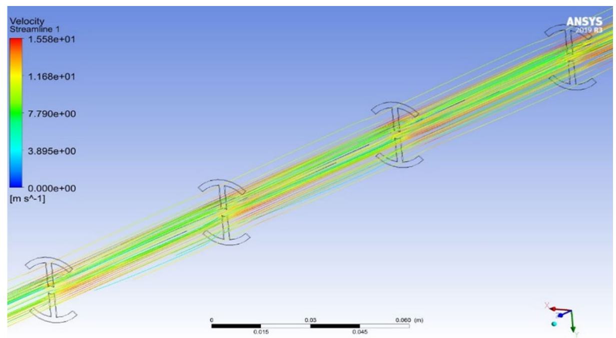
	45°	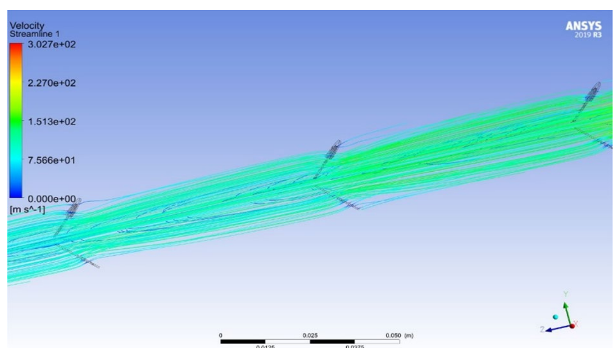
	30°	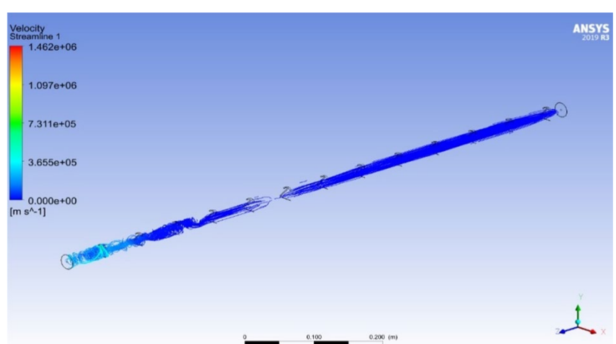

Table 3 (continued)

P/D ratio	MIs angle	
P/D = 4	90°	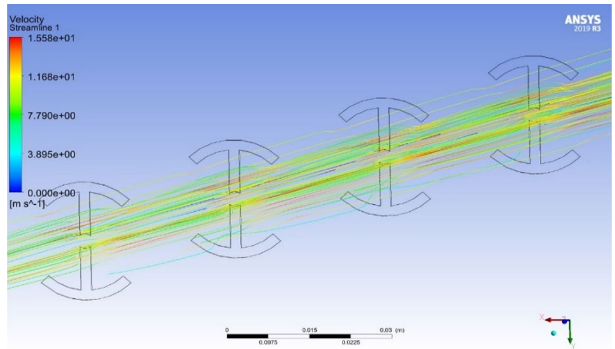
	45°	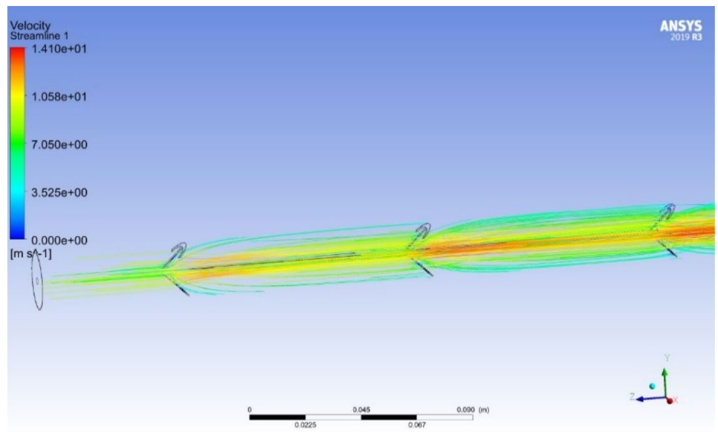
	30°	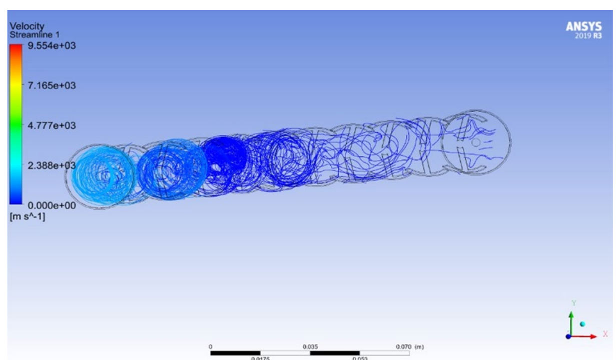
P/D = 6	90°	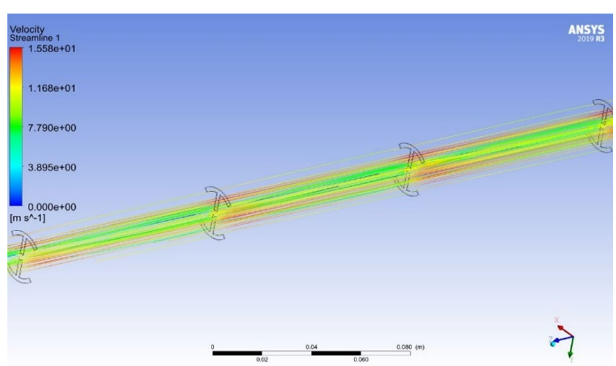

Table 3 (continued)

P/D ratio	MIs angle	
	45°	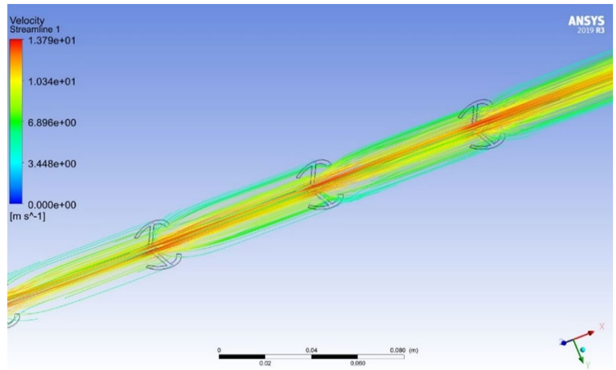
	30°	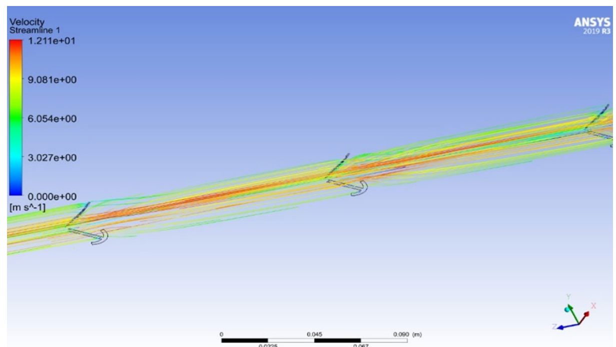

Acknowledgements We would like to mention that, this work is not funded by any external or internal agency. We are deeply grateful to JSPM Narhe Technical Campus, Pune for providing a platform for CFD analysis, Visvesvaraya National Institute of Technology for providing a platform for Experimentation and G. H. Raisoni College of Engineering, Nagpur for providing a platform for Plagiarism checking.

Funding This research work has been carried out without any funding from internal as well as external agencies.

Availability of data and material This manuscript has no associated data or the data will not be deposited.

Declarations

Conflict of interest On behalf of all authors, the corresponding author states that there is no conflict of interest.

References

1. Mousa MH, Miljkovic N, Nawaz K (2021) Review of heat transfer enhancement techniques for single phase flows. Renew Sustain Energy Rev 137:110566. https://doi.org/10.1016/j.rser.2020.110566
2. Webb RL, Eckert ERG, Goldstein RJ (1971) Heat transfer and friction in tubes with repeated-rib roughness. Int J Heat Mass Transf 14:601–617. https://doi.org/10.1016/0017-9310(71)90009-3
3. Fiebig M (1995) Embedded vortices in internal flow: heat transfer and pressure loss enhancement. Int J Heat Fluid Flow 16:376–388
4. Manglik RM, Bergles AE (1993) Heat transfer and pressure drop correlations for twisted-tape inserts in isothermal tubes: part II—Transition and turbulent flows. J Heat Transfer 115:890–896. https://doi.org/10.1115/1.2911384
5. Eiamsa-ard S, Thianpong C, Promvonge P (2006) Experimental investigation of heat transfer and flow friction in a circular tube fitted with regularly spaced twisted tape elements. Int Commun Heat Mass Transf 33:1225–1233. https://doi.org/10.1016/j.icheatmasstransfer.2006.08.002
6. Naphon P, Suwagrai J (2007) Effect of curvature ratios on the heat transfer and flow developments in the horizontal spirally coiled tubes. Int J Heat Mass Transf 50:444–451. https://doi.org/10.1016/j.ijheatmasstransfer.2006.08.002

7. Nag S, Rao MR (1987) Forced convection heat transfer in smooth tubes roughened by helically coiled ribbons. Int J Heat Mass Transf 30:1541–1544. https://doi.org/10.1016/0017-9310(87)90186-4
8. Wang L, Sundén B (2002) Performance comparison of some tube inserts. Int Commun Heat Mass Transf 29:45–56. https://doi.org/10.1016/S0735-1933(01)00323-2
9. Fiebig M, Kallweit P, Mitra N, Tiggelbeck S (1991) Heat transfer enhancement and drag by longitudinal vortex generators in channel flow. Exp Therm Fluid Sci 4:103–114. https://doi.org/10.1016/0894-1777(91)90024-L
10. Yakut K, Sahin B, Celik C et al (2005) Effects of tapes with double-sided delta-winglets on heat and vortex characteristics. Appl Energy 80:77–95. https://doi.org/10.1016/j.apenergy.2004.03.003
11. Akhavan-Behabadi MA, Mohseni SG, Najafi H, Ramazanzadeh H (2009) Heat transfer and pressure drop characteristics of forced convective evaporation in horizontal tubes with coiled wire inserts. Int Commun Heat Mass Transf 36:1089–1095. https://doi.org/10.1016/j.icheatmasstransfer.2009.07.009
12. Rambhad KS, Walke PV (2018) Regeneration of composite desiccant dehumidifier by parabolic trough solar collector : an experimental investigation. Mater Today Proc 5:24358–24366. https://doi.org/10.1016/j.matpr.2018.10.231
13. Rambhad KS, Walke PV (2017) An experimental investigation of solar assisted air heating for solid desiccant regeneration using parabolic trough solar concentrator. Int J Anal Exp Finite Elem Anal 4:45–47
14. Huang ZF, Nakayama A, Yang K et al (2010) Enhancing heat transfer in the core flow by using porous medium insert in a tube. Int J Heat Mass Transf 53:1164–1174. https://doi.org/10.1016/j.ijheatmasstransfer.2009.10.038
15. Naphon P, Suchana T (2011) Heat transfer enhancement and pressure drop of the horizontal concentric tube with twisted wires brush inserts. Int Commun Heat Mass Transf 38:236–241. https://doi.org/10.1016/j.icheatmasstransfer.2010.11.018
16. Bas H, Ozceyhan V (2012) Heat transfer enhancement in a tube with twisted tape inserts placed separately from the tube wall. Exp Therm Fluid Sci 41:51–58. https://doi.org/10.1016/j.expthermflusci.2012.03.008
17. Salam B, Biswas S, Saha S, Bhuiya MMK (2013) Heat transfer enhancement in a tube using rectangular-cut twisted tape insert. Procedia Eng 56:96–103. https://doi.org/10.1016/j.proeng.2013.03.094
18. Eiamsa-Ard S, Kiatkittipong K (2014) Heat transfer enhancement by multiple twisted tape inserts and TiO 2/water nanofluid. Appl Therm Eng 70:896–924. https://doi.org/10.1016/j.applthermaleng.2014.05.062
19. Zheng ZJ, Li MJ, He YL (2015) Optimization of porous insert configurations for heat transfer enhancement in tubes based on genetic algorithm and CFD. Int J Heat Mass Transf 87:376–379. https://doi.org/10.1016/j.ijheatmasstransfer.2015.04.016
20. Haskins DA, El-Genk MS (2016) CFD analyses and correlation of pressure losses on the shell-side of concentric, helically-coiled tubes heat exchangers. Nucl Eng Des 305:531–546. https://doi.org/10.1016/j.nucengdes.2016.05.014
21. Meinicke S, Wetzel T, Dietrich B (2017) Scale-resolved CFD modelling of single-phase hydrodynamics and conjugate heat transfer in solid sponges. Int J Heat Mass Transf 108:1207–1219. https://doi.org/10.1016/j.ijheatmasstransfer.2016.12.052
22. Sharifi K, Sabeti M, Rafiei M et al (2018) Computational fluid dynamics (CFD) technique to study the effects of helical wire inserts on heat transfer and pressure drop in a double pipe heat exchanger. Appl Therm Eng 128:898–910. https://doi.org/10.1016/j.applthermaleng.2017.08.146
23. Tusar M, Ahmed K, Bhuiya M et al (2019) CFD study of heat transfer enhancement and fluid flow characteristics of laminar flow through tube with helical screw tape insert. Energy Proced 160:699–706
24. Pandey L, Prajapati H, Singh S (2020) CFD study for enhancement of heat transfer and flow characteristics of circular tube heat exchanger using Y-shaped insert. Mater Today Proc. https://doi.org/10.1016/j.matpr.2020.10.890
25. Dang W, Wang LB (2021) Convective heat transfer enhancement mechanisms in circular tube inserted with a type of twined coil. Int J Heat Mass Transf 169:120960. https://doi.org/10.1016/j.ijheatmasstransfer.2021.120960
26. Wijayanta AT, Istanto T, Kariya K, Miyara A (2017) Heat transfer enhancement of internal flow by inserting punched delta winglet vortex generators with various attack angles. Exp Therm Fluid Sci 87:141–148. https://doi.org/10.1016/j.expthermflusci.2017.05.002
27. Chokphoemphun S, Pimsarn M, Thianpong C, Promvonge P (2015) Heat transfer augmentation in a circular tube with winglet vortex generators. Chin J Chem Eng 23:605–614. https://doi.org/10.1016/j.cjche.2014.04.002
28. Liu Hn-l, Li H, He Y-l, Chen Z-t (2018) Heat transfer and flow characteristics in a circular tube fitted with rectangular winglet vortex generators. Int J Heat Mass Transf 126:989–1006. https://doi.org/10.1016/j.ijheatmasstransfer.2018.05.038
29. Awais M, Bhuiyan AA (2018) Heat transfer enhancement using different types of vortex generators (VGs): a review on experimental and numerical activities. Therm Sci Eng Prog 5:524–545
30. Gallegos RKB, Sharma RN (2017) Flags as vortex generators for heat transfer enhancement: gaps and challenges. Renew Sustain Energy Rev 76:950–962
31. Mahanthesh B, Shashikumar NS, Lorenzini G (2020) Heat transfer enhancement due to nanoparticles, magnetic field, thermal and exponential space-dependent heat source aspects in nanoliquid flow past a stretchable spinning disk. J Therm Anal Calorim. https://doi.org/10.1007/s10973-020-09927-x
32. Rasool G, Shafiq A (2020) Numerical exploration of the features of thermally enhanced chemically reactive radiative Powell-Eyring nanofluid flow via darcy medium over non-linearly stretching surface affected by a transverse magnetic field and convective boundary conditions. Appl Nanosci. https://doi.org/10.1007/s13204-020-01625-2
33. Rasool G, Shafiq A, Baleanu D (2020) Consequences of soret-dufour effects, thermal radiation, and binary chemical reaction on darcy forchheimer flow of nanofluids. Symmetry (Basel) 12:1–19. https://doi.org/10.3390/SYM12091421